Orion Entry Performance-Based Center-of-Gravity Box

Jeremy R. Rea *

NASA Johnson Space Center, Houston, Texas, 77058

The Orion capsule has many performance requirements for its atmospheric entry trajectory. Requirements on landing accuracy, maximum heating rate, total heat load, propellant usage, and sensed acceleration must all be satisfied. It is desired to define a methodology to translate the many performance requirements for an atmospheric entry trajectory into language easily understood by vehicle designers in terms of an allowable center-of-gravity box. This is possible by noting that most entry performance parameters for a capsule vehicle are mainly determined by the lift-to-drag ratio of the vehicle. However, the lift-to-drag ratio should be considered a probabilistic quantity rather than deterministic, where variations in the lift-to-drag are caused by both aerodynamic and center-of-gravity uncertainties. This paper discusses the technique used by the Orion program to define the allowable dispersions in center-of-gravity to achieve the desired entry performance while accounting for aerodynamic uncertainty.

Nomenclature

CFD	Computational Fluid Mechanics
CG	Center-of-Gravity
ISS	International Space Station
LEO	Low Earth Orbit
MRC	Moment Reference Center
TPS	Thermal Protection System
A_{ref}	Reference area
C_A	Axial force coefficient
C_D	Drag coefficient
C_L	Lift coefficient
C_N	Normal force coefficient
C_m	Pitching moment coefficient about CG
C_{m_o}	Pitching moment coefficient about MRC
C_{m_α}	partial derivative of C_m with respect to angle of attack
D	Aerodynamic drag force
L	Aerodynamic lift force
L/D	Lift-to-Drag ratio
L_{ref}	Reference length
M	Mach number
V	Atmospheric relative velocity
X_{CG}	X-component of CG
X_{MRC}	X-component of MRC
Z_{CG}	Z-component of CG
Z_{MRC}	Z-component of MRC
ΔX_{CG}	$(X_{CG} - X_{MRC})$
ΔZ_{CG}	$(Z_{CG} - Z_{MRC})$
α	Angle of attack
α_{trim}	Trim angle of attack

*Subsystem Manager, Flight Mechanics and Trajectory Design Branch, 2101 NASA Parkway - EG5, AIAA Member.

γ_{EI}	Flight path angle at entry interface
ρ	Atmospheric density

I. Introduction

The Orion vehicle is designed both for Low Earth Orbit (LEO) missions to the International Space Station (ISS) and for missions to the moon.[1–3] It is a capsule-type vehicle with a lift-to-drag (L/D) ratio in the range of 0.25-0.27. For ISS class missions, the capsule will use an Apollo-style direct entry. For lunar return missions, depending on the timing of the mission, the capsule could perform a direct entry or a skip entry of up to 4800 n.mi. in order to land in the coastal waters of California.

The physics of atmospheric re-entry determine the capability of the Orion vehicle. For the given vehicle mass and capsule shape, the driving parameters of the entry trajectory are the hypersonic L/D and the flight path angle at entry interface (γ_{EI}). The design of the Orion atmospheric re-entry must meet constraints during both nominal and dispersed flight conditions on landing accuracy, maximum heat rate, total heat load, sensed acceleration, and proper disposal of both the Docking Module and Service Module.[4] These constraints define an entry corridor in the space of L/D-γ_{EI}; if the vehicle falls within this corridor, then all constraints are met. The γ_{EI} dimension of the corridor is further constrained by the debris disposal considerations. Thus, the entry performance for the Orion vehicle can be described almost completely by the L/D.[5]

The L/D is a function of both the aerodynamics and the center-of-gravity (CG) of the vehicle. The aerodynamics of the vehicle are determined by Computational Fluid Mechanics (CFD) and wind tunnel tests. However, the aerodynamics are not known precisely. Instead, an aerodynamic database has been developed where the aerodynamic coefficients are known to fall within a probabilistic band defined by upper and lower bounds.[6] It is expected that the probabilistic band will shrink after the first missions are flown and real-world data is collected. Until that time, the Orion must be designed to the pre-flight aerodynamic database.

Bounds on the hypersonic L/D necessary to achieve all the mission requirements can be defined for the given entry corridor. In order to achieve the desired landing accuracy, a minimum L/D must be ensured. The design of the Thermal Protection System (TPS) drives the upper limit. A higher L/D can drive mass into the design of the TPS. Conversely, once the TPS is designed, the L/D must be ensured to stay below a certain limit in order for the TPS to stay within its design envelop. The L/D must stay within its upper and lower bounds during dispersed flight conditions. For a given aerodynamic database with given uncertainties, the allowable range in L/D can be mapped to an allowable box for the CG location. The CG box is used to set requirements on the dispersions allowed for vehicle packaging and cargo storage. As the aerodynamic uncertainties decrease, the size of the CG box can increase. This paper discusses the technique used to map the minimum and maximum L/D bounds set by the entry performance requirements to the allowable dispersions in CG while accounting for aerodynamic uncertainties.

II. Contributors to Variation in Hypersonic Lift-to-Drag

The aerodynamic lift force (L) and aerodynamic drag force (D) on the vehicle are nonlinear functions of the position, velocity, and attitude.

$$L = \frac{1}{2}\rho V^2 A_{ref} C_L \tag{1}$$

$$D = \frac{1}{2}\rho V^2 A_{ref} C_D \tag{2}$$

where

ρ	=	Atmospheric density
V	=	Atmospheric relative velocity
A_{ref}	=	Reference area
C_L	=	Lift coefficient
C_D	=	Drag coefficient

The L/D is defined as the ratio of the aerodynamic lift force to the aerodynamic drag force. It is equivalent to the ratio of C_L over C_D. This relationship is shown in equation 3.

$$\frac{L}{D} = \frac{C_L(M, \alpha)}{C_D(M, \alpha)} \tag{3}$$

C_L and C_D are functions of Mach number (M) and angle of attack (α). A Mach number of 25 is used as a measuring point of the hypersonic L/D. Figure 1 shows the hypersonic C_L and C_D as a function of the angle of attack. The nominal value of C_L is shown as a dotted red line, and the nominal value of C_D is shown as a solid blue line. The shaded regions show the uncertainty bands about each nominal value.

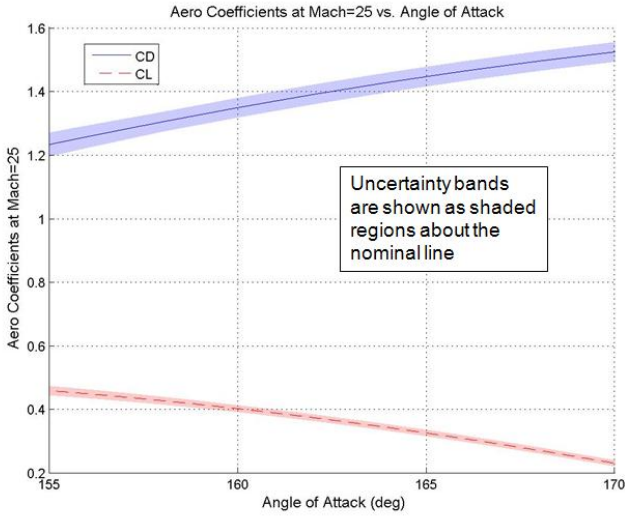

Figure 1. Hypersonic Lift and Drag Coefficients versus Angle of Attack

Figure 2 shows the hypersonic L/D as a function of the angle of attack. The solid line shows the nominal value, and the shaded region shows the uncertainty band about the nominal. Red x's show the hypersonic L/D values from a monte carlo simulation with uniformly distributed uncertainties on C_L, C_D, and the center-of-gravity.

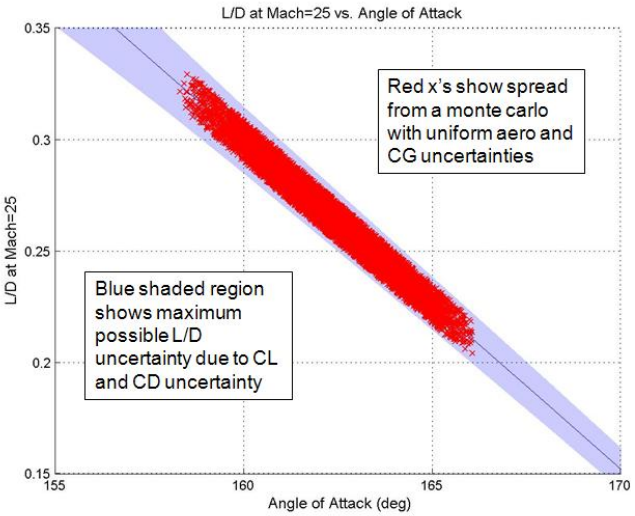

Figure 2. Hypersonic Lift-to-Drag Ratio versus Angle of Attack

From Figure 2 it can be seen that variations in L/D are caused by variations in C_L, C_D, and α. This is shown mathematically in equation 4. Figure 3 graphically points out the effect of each contribution to the

total L/D variation. For the example data shown, the combined variations in C_L and C_D contribute to a L/D variation of roughly ± 0.01. However, most of the variation in L/D comes from variation in the angle of attack; here the angle of attack variation contributes a variation in L/D of roughly ± 0.06.

$$\delta\left(\frac{L}{D}\right) = \left[-\frac{C_L}{C_D^2}\right]\delta C_D + \left[\frac{1}{C_D}\right]\delta C_L + \left[\frac{\partial\left(L/D\right)}{\partial\alpha}\right]\delta\alpha \tag{4}$$

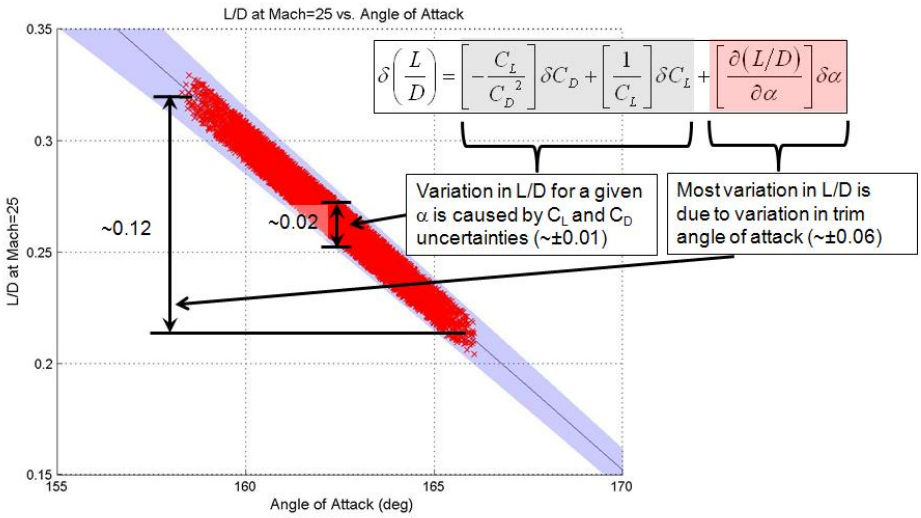

Figure 3. Hypersonic Lift-to-Drag Ratio versus Angle of Attack

III. Contributors to Variation in Trim Angle of Attack

The vehicle is trimmed when the aerodynamic moments are balanced. The trim angle of attack (α_{trim}) is defined when the pitching moment coefficient (C_m) is zero. Equation 5 defines the partial derivative of C_m with respect to angle of attack as C_{m_α}.

$$C_{m_\alpha}\left(M,\alpha\right) = \frac{\partial C_m}{\partial\alpha} \approx \frac{\delta C_m}{\delta\alpha} \tag{5}$$

Applying this equation at α_{trim} and rearranging gives a relationship between variations in C_m and α_{trim}.

$$\delta\alpha_{trim} = \left[\frac{1}{C_{m_\alpha}\left(M,\alpha_{trim}\right)}\right]\delta C_m \tag{6}$$

C_m is related to α , the X-component of CG (X_{CG}), and the Z-component of CG (Z_{CG}) by equation 7.

$$C_m = C_{m_o}\left(M,\alpha\right) - C_A\left(M,\alpha\right)\frac{\Delta Z_{CG}}{L_{ref}} + C_N\left(M,\alpha\right)\frac{\Delta X_{CG}}{L_{ref}} \tag{7}$$

where

$$\begin{aligned}
C_m &= \text{Pitching coefficient about CG}\\
C_{m_o} &= \text{Pitching coefficient about Moment Reference Center (MRC)}\\
C_N &= \text{Normal force coefficient}\\
C_A &= \text{Axial force coefficient}\\
\Delta X_{CG} &= \left(X_{CG} - X_{MRC}\right)\\
\Delta Z_{CG} &= \left(Z_{CG} - Z_{MRC}\right)\\
L_{ref} &= \text{Reference length}
\end{aligned}$$

Equation 8 shows that variations in C_{m_o}, X_{CG}, and Z_{CG} cause variation in α_{trim}. For the Orion capsule, C_{m_o} and Z_{CG} uncertainties are the major contributors to α_{trim} variation and thus to L/D variation.

$$\delta\alpha_{trim} = \frac{1}{C_{m_\alpha}(M, \alpha_{trim})}\left[\delta C_{m_o} - \frac{C_A(M, \alpha_{trim})}{L_{ref}}\delta Z_{CG} + \frac{C_N(M, \alpha_{trim})}{L_{ref}}\delta X_{CG}\right] \tag{8}$$

Figure 4 shows a plot of C_m as a function of α. The solid black line is the nominal value of C_m. The red, yellow, and blue shaded regions show the variation in C_m due to uncertainties in X_{CG}, Z_{CG}, and C_{m_o}, respectively. The trim line for $C_m = 0$ is shown. Along this trim line, the variation in trim angle of attack due to X_{CG}, Z_{CG}, and C_{m_o} can be seen. The C_{m_o} and Z_{CG} uncertainties each cause roughly $\pm 1.8^o$ deg variation in trim angle of attack, while the X_{CG} uncertainty causes only $\pm 0.3^o$. Trim angle of attack variations of $\pm 1.8^o$ and $\pm 0.3^o$ translate into L/D variations of ± 0.0275 and ± 0.0025, respectively.

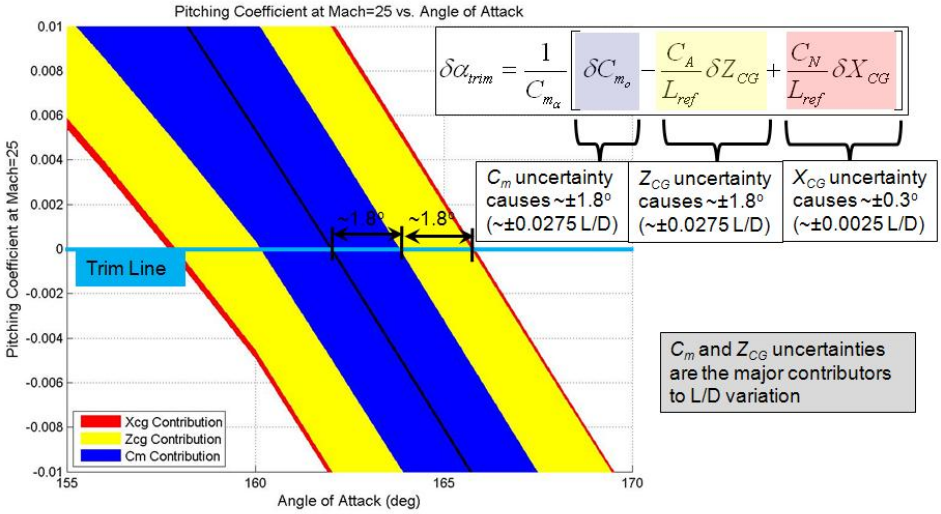

Figure 4. Hypersonic Pitching Coefficient versus Angle of Attack

IV. Entry Performance-Based Center-of-Gravity Box

It is possible to define bounds on the L/D which must be achieved in order to meet various entry performance requirements. For the Orion vehicle, extensive analysis has been completed which shows that the minimum allowable L/D for meeting the landing accuracy requirements for an ISS return mission is 0.20.[7] This is the minimum allowable L/D in the presence of all environmental and vehicle uncertainties. An upper bound on L/D can be determined by heating constraints on the heat shield. For ISS return missions, the heating environment does not place a strong constraint on L/D. For this reason, engineering judgment was used to pick an upper limit of 0.32.

The L/D limits can now be translated into a center-of-gravity box. For a given Mach number, a desired L/D value can be achieved with a specific value of α_{trim}. Applying equation 7 at the trim angle of attack results in equation 9.

$$0 = C_{m_o}(M, \alpha_{trim}) - C_A(M, \alpha_{trim})\frac{\Delta Z_{CG}}{L_{ref}} + C_N(M, \alpha_{trim})\frac{\Delta X_{CG}}{L_{ref}} \tag{9}$$

For a given Mach number and α_{trim}, equation 9 defines a linear relationship between the X_{CG} and Z_{CG} . Thus, a line of constant L/D can be drawn on the vehicle in the XZ-plane. If the CG lies on this line, then the desired L/D will be achieved. When aerodynamic uncertainties are considered, the line of constant L/D expands into a probability band of constant L/D. If the CG falls within this probability band, then there is a chance that the desired L/D will be achieved.

Figure 5 shows an example of the entry performance-based CG box for ISS returns. The horizontal axis of the figure represents the X_{CG} location along the axis of the capsule, and the vertical axis of the figure

represents the Z_{CG} location off the axis of the capsule. The blue and red bands show the L/D probability bands. The blue band shows the region where it is possible to achieve the minimum L/D for entry landing accuracy performance. The red band shows the region where it is possible to achieve the maximum L/D for entry TPS performance. The lines inside each band represent contours of probability. Each line represents a 5% increase in the chance that the L/D will be outside its maximum or minimum bound. The dotted black line shows a nominal L/D=0.25 line for nominal aerodynamics with no uncertainties. On this line is shown a typical CG dispersion. Each concentric ellipse represents a Gaussian distribution on CG at a probability level of 1-sigma, 2-sigma, or 3-sigma. This figure is a graphical representation of the methodology used to define the allowable CG dispersions for the Orion vehicle.

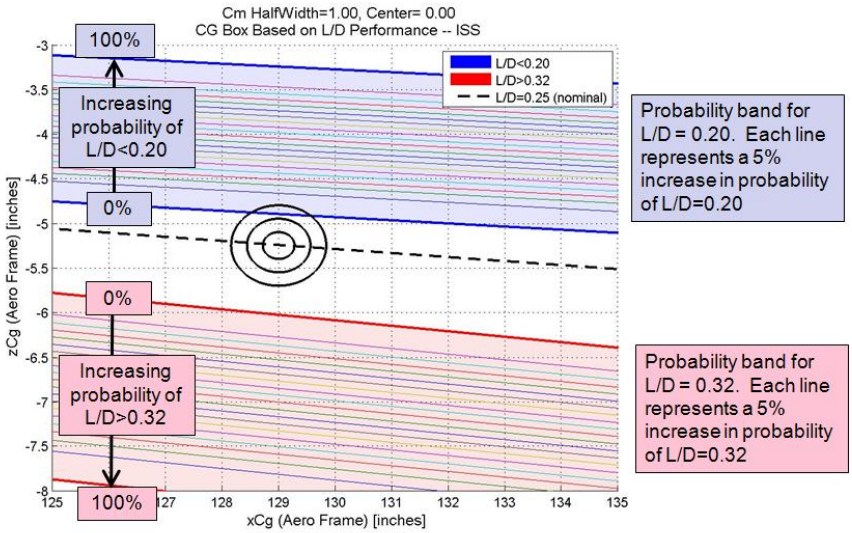

Figure 5. Entry Performance-Based CG Box for ISS Return Mission

For the CG box in Figure 5, there is a slight chance that the L/D can be below the minimum desired value of 0.20. In order to build robustness into the vehicle design, it is desired to limit the 3-sigma CG dispersions to keep them from intersecting the upper and lower L/D probability bands. Care must be taken to choose both the mean and 3-sigma CG values in order to meet the entry performance requirements. Figure 6 shows the trade-off between the nominal L/D and the maximum allowable Z_{CG} dispersion. On the horizontal axis is the maximum allowable Z_{CG} dispersion. On the left vertical axis is the nominal L/D, and on the right vertical axis is the corresponding value of nominal Z_{CG}. This line is taken at an assumed X_{CG} value of 128 inches. For a desired 3-sigma Z_{CG} dispersion of 0.45 inches with no possibility of an L/D less than 0.20, the nominal L/D must be 0.2541. This CG box is shown in Figure 7.

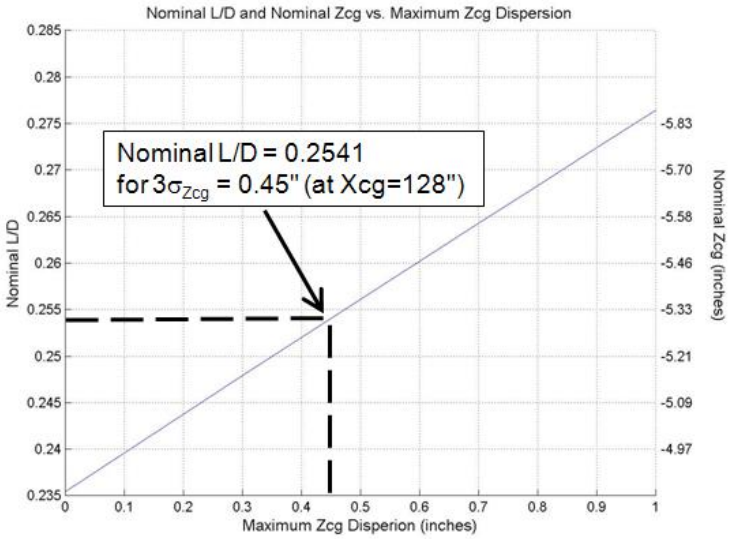

Figure 6. Trade Between Nominal L/D and Maximum Z_{CG} Dispersion

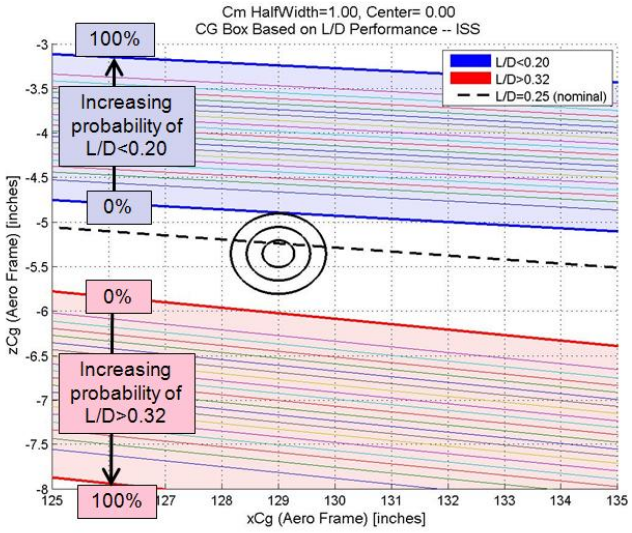

Figure 7. Entry Performance-Based CG Box for ISS Return Mission – Updated

V. Effect of Aerodynamic Uncertainty Reduction

This methodology can also be used to investigate the effect of aerodynamic uncertainty reduction on the performance-based CG box. It is expected that after the first flights of the Orion capsule, flight data can be used to reduce the aerodynamic uncertainties. However, the uncertainty reductions may not occur symmetrically about the nominal values. The reductions may manifest as not only a reduction in the uncertainty about a nominal value, but also a shift in the nominal value. Figure 8 shows an example where the uncertainties on C_{m_o} are reduced symmetrically by 50%. This causes a roughly 50% reduction in trim angle of attack variation due to C_{m_o} from $\pm 1.8^o$ to $\pm 0.9^o$. This reduction in trim angle of attack variation leads to a reduction in L/D variation from ± 0.0275 to ± 0.0138. Figure 9 shows an example where the uncertainty on C_{m_o} is reduced by 50% but the nominal is increased by 50%. The variation in trim angle of attack and L/D are still reduced by the same amount, but now the nominal values are shifted. The nominal L/D value is biased down by 0.0138. Figure 10 shows another example where the uncertainty on C_{m_o} is reduced by 50% but the nominal is decreased by 50%. This leads to the nominal L/D being biased up by 0.0138.

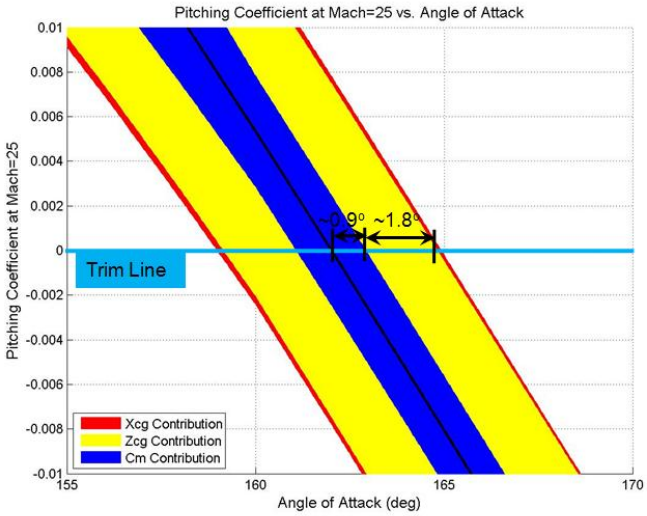

Figure 8. Hypersonic Pitching Coefficient versus Angle of Attack – 50% Uncertainty Reduction with No Shift in Nominal

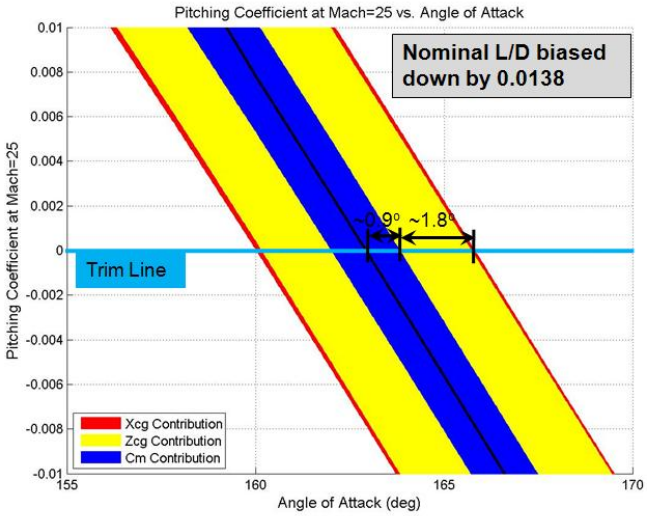

Figure 9. Hypersonic Pitching Coefficient versus Angle of Attack – 50% Uncertainty Reduction with 50% Increase in Nominal

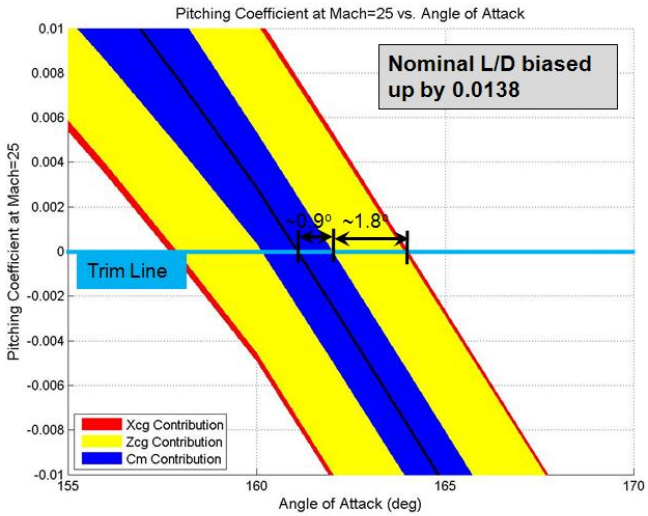

Figure 10. Hypersonic Pitching Coefficient versus Angle of Attack – 50% Uncertainty Reduction with 50% Decrease in Nominal

This same type of aerodynamic uncertainty reduction can be plotted in the CG-space. Figure 11 shows the case where the C_{m_o} uncertainties are reduced by 25% with no shift in the nominal value. Figure 12 shows the case where the C_{m_o} uncertainties are reduced by 25% and the nominal value is increased by 25%. For the Orion capsule, ballast mass is required in order to achieve the desired Z_{CG} offset. In this case, more ballast will be required in order to maintain the same nominal L/D. Figure 13 shows the case where the C_{m_o} uncertainties are reduced by 25% and the nominal value is decreased by 25%. In this case, less ballast is required to achieve the same nominal L/D. Note that for all cases, the width of the allowable CG box increases due to the reduced aerodynamic uncertainties.

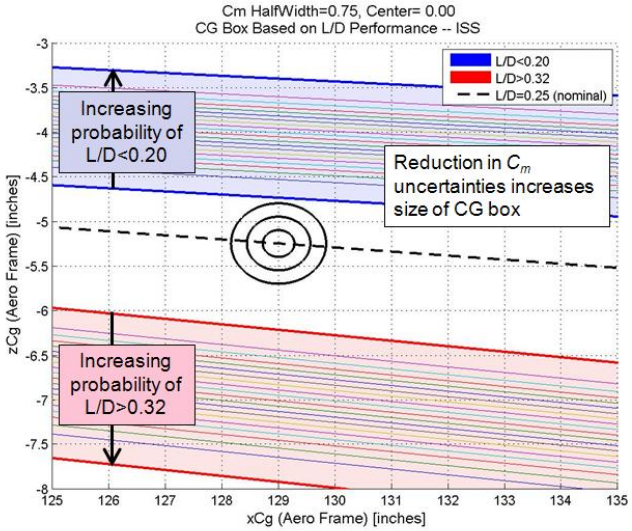

Figure 11. Entry Performance-Based CG Box for ISS Return Mission – 25% C_m Uncertainty Reduction with No Shift in Nominal

VI. Summary

Entry performance is a complex problem with many requirements. For low-L/D capsule-shaped vehicles, much of the entry performance can be put in terms of the L/D. Entry performance is determined by not only the nominal value of L/D, but also by the variation about the nominal. The L/D (and thus the entry

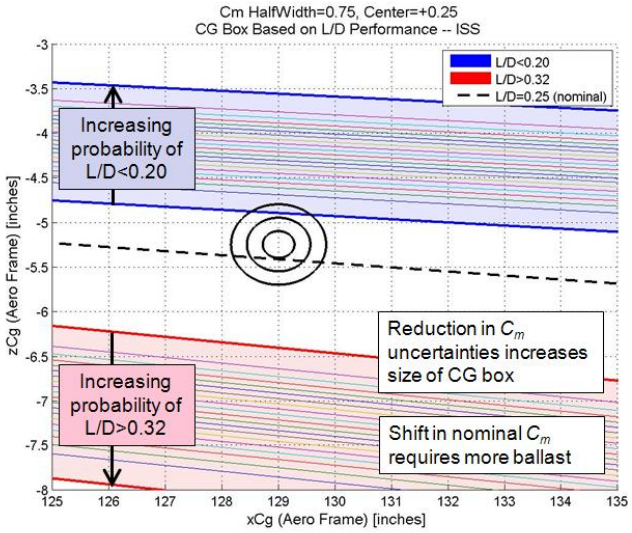

Figure 12. Entry Performance-Based CG Box for ISS Return Mission – 25% C_m Uncertainty Reduction with 25% Increase in Nominal C_m

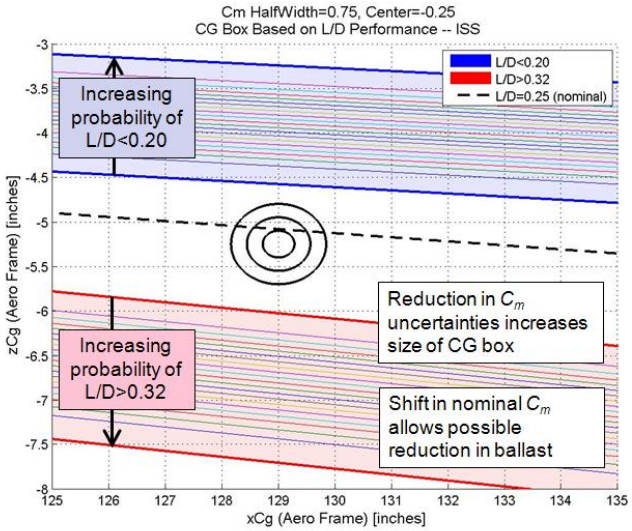

Figure 13. Entry Performance-Based CG Box for ISS Return Mission – 25% C_m Uncertainty Reduction with 25% Decrease in Nominal C_m

performance) is a highly complex function of aerodynamics and CG. In the design of a vehicle, neither of these parameters are deterministic, but are rather probabilistic. In order that the vehicle remain robust to uncertainties in the operating environment and the vehicle parameters themselves, it is important to understand the interaction between all these factors. The methodology discussed in this paper has been used by the Orion program to define the requirements on the CG box while accounting for aerodynamic uncertainty. In addition, it has been used to determine how a reduction in aerodynamic uncertainty may affect the ballast mass necessary to achieve the desired entry performance.

Acknowledgments

Many people have contributed to the work presented in this paper including Tim Crull and Luke McNamara of the Johnson Space Center, and Zach Putnam and Mark Jackson of the Charles Stark Draper Laboratory. The author would also like to recognize the technical achievements of the original Apollo engineers.

References

[1]Broome, J. M. and Johnson, W., "Orion Entry, Descent, and Landing Performance and Mission Design," *AIAA Guidance, Navigation and Control Conference and Exhibit*, American Institute of Aeronautics and Astronautics, Inc., Hilton Head, SC, Aug. 2007, AIAA-2007-6430.

[2]Chambers, R. P., "Seven Spacecraft in One – Orion Guidance, Navigation, and Control," *AIAA SPACE 2008 Conference & Exposition*, American Institute of Aeronautics and Astronautics, Inc., San Diego, CA, Sept. 2008, AIAA-2008-7744.

[3]Rea, J. R., "A Comparison of Two Orion Skip Entry Guidance Algorithms," *AIAA Guidance, Navigation and Control Conference and Exhibit*, American Institute of Aeronautics and Astronautics, Inc., Hilton Head, SC, Aug. 2007, AIAA-2007-6424.

[4]Rea, J. R., "Orion Entry Flight Corridor Analysis," *AIAA Guidance, Navigation and Control Conference and Exhibit*, American Institute of Aeronautics and Astronautics, Inc., Honolulu, HI, Aug. 2008, AIAA-2008-7153.

[5]McNamara, L., "DAC3 Entry Corridor for Lunar and LEO Returns," Tech. Rep. FltDyn-CEV-09-84, NASA Johnson Space Center, Houston, TX, June 2009.

[6]"Orion Aerodynamic Databook, Ver 0.55.1, Volume 1," Tech. Rep. NASA CXP-72167, NASA Johnson Space Center, Houston, TX, May 2010.

[7]Crull, T., "Determination of Minimum L/D for ISS Entry," Tech. Rep. FltDyn-CEV-09-155, NASA Johnson Space Center, Houston, TX, 2009.